Imaging Science in Dentistry 2022; 52: 245-58
https://doi.org/10.5624/isd.20220019

CBCT-based assessment of root canal treatment using micro-CT reference images

Alessando Lamira[1], Jardel Francisco Mazzi-Chaves[1], Laura Ferreira Pinheiro Nicolielo[2], Graziela Bianchi Leoni[3], Alice Corrêa Silva-Sousa[1], Yara Terezinha Corrêa Silva-Sousa[3], Ruben Pauwels[2,4,5], Nico Buls[6], Reinhilde Jacobs[2,7], Manoel Damião Sousa-Neto[1,*]

[1]*Department of Restorative Dentistry, School of Dentistry of Ribeirão Preto, University of São Paulo, Brazil*
[2]*OMFS IMPATH Research Group, Department of Imaging and Pathology, Faculty of Medicine, University of Leuven, University Hospitals Leuven, Leuven, Belgium*
[3]*Faculty of Dentistry, University of Ribeirão Preto, Ribeirão Preto, Brazil*
[4]*Department of Radiology, Faculty of Dentistry, Chulalongkorn University, Bangkok, Thailand*
[5]*Aarhus Institute of Advanced Studies, Aarhus University, Aarhus, Denmark*
[6]*Department of Radiology, Universitair Ziekenhuis Brussel, Vrije Universiteit Brussel, Brussels, Belgium*
[7]*Department of Dental Medicine, Karolinska Institutet, Stockholm, Sweden*

ABSTRACT

Purpose: This study compared the root canal anatomy between cone-beam computed tomography (CBCT) and micro-computed tomography (micro-CT) images before and after biomechanical preparation and root canal filling.
Materials and Methods: Isthmus-containing mesial roots of mandibular molars (n = 14) were scanned by micro-CT and 3 CBCT devices: 3D Accuitomo 170 (ACC), NewTom 5G (N5G) and NewTom VGi evo (NEVO). Two calibrated observers evaluated the images for 2-dimensional quantitative parameters, the presence of debris or root perforation, and filling quality in the root canal and isthmus. The kappa coefficient, analysis of variance, and the Tukey test were used for statistical analyses ($\alpha = 5\%$).
Results: Substantial intra-observer agreement ($\kappa = 0.63$) was found between micro-CT and ACC, N5G, and NEVO. Debris detection was difficult using ACC (42.9%), N5G (40.0%), and NEVO (40%), with no agreement between micro-CT and ACC, N5G, and NEVO ($0.05 < \kappa < 0.12$). After biomechanical preparation, 2.4%-4.8% of CBCT images showed root perforation that was absent on micro-CT. The 2D parameters showed satisfactory reproducibility between micro-CT and ACC, N5G, and NEVO (intraclass correlation coefficient: 0.60-0.73). Partially filled isthmuses were observed in 2.9% of the ACC images, 8.8% of the N5G and NEVO images, and 26.5% of the micro-CT images, with no agreement between micro-CT and ACC, and poor agreement between micro-CT and N5G and NEVO. Excellent agreement was found for area, perimeter, and the major and minor diameters, while the roundness measures were satisfactory.
Conclusion: CBCT images aided in isthmus detection and classification, but did not allow their classification after biomechanical preparation and root canal filling. ***(Imaging Sci Dent 2022; 52: 245-58)***

KEY WORDS: Cone-Beam Computed Tomography, X-Ray Microtomography, Endodontics

Introduction

Intraoral radiographs and cone-beam computed tomography (CBCT) scans are essential tools for diagnosis and treatment planning in endodontics. For CBCT, small fields of view (FOVs) are most often indicated in endodontics, since they allow higher resolution and a lower radiation dose, while providing a smaller volume of data to be inter-

We gratefully acknowledge financial support from the Coordination for the Improvement of Higher Education Personnel (CAPES-Brazil process no. 33002029032P4) and the São Paulo Research Foundation (process no. 2018/14450-1). Ruben Pauwels is supported by the European Union Horizon 2020 Research and Innovation Programme under the Marie Skłodowska-Curie grant agreement number 754513 and by Aarhus University Research Foundation (AIAS-COFUND).
Received January 25, 2022; Revised March 31, 2022; Accepted April 8, 2022
Published online May 13, 2022
*Correspondence to : Prof. Manoel Damião Sousa-Neto
Department of Restorative Dentistry, School of Dentistry of Ribeirão Preto, University of São Paulo, 350 Célia de Oliveira Meirelles Street, Ribeirão Preto, São Paulo 14024-070, Brazil
Tel) 55-16-3315-3982, E-mail) sousanet@forp.usp.br

Imaging Science in Dentistry · pISSN 2233-7822 eISSN 2233-7830

preted.[1-3] After image reconstruction, CBCT software allows dynamic navigation in multiple planes, enabling quantitative 2-dimensional (2D) and 3-dimensional (3D) measurements regarding length, area, perimeter, and volume, aiding in the diagnosis and planning of endodontic treatment.[1,2] At present, the use of CBCT in this field has been shown to be effective for detecting pathological conditions such as fractures and resorptions, determining the location and extension of periapical lesions, evaluating perforations, and investigating additional/accessory canals and roots.[1-5]

Micro-computed tomography (micro-CT) scanners are often used in laboratory research and have similar general characteristics to CBCT devices (e.g., beam shape and a flat panel detector), but micro-CT involves a smaller FOV, a higher radiation dose, a longer scanning time, and a critical hardware setup.[6-8] Although micro-CT scanners are not clinically applicable, several aspects regarding the use of CBCT have been developed and improved based on knowledge gained from micro-CT. For endodontics, the use of high-resolution 3D data has facilitated a better understanding of anatomical challenges, such as flattening, curvature, lateral and accessory canals, apical deltas, and isthmuses, as well as the cleaning, shaping and filling procedures of the root canal system (RCS),[5,8,9] offering better insights into anatomy, pathology, and anticipated endodontic strategies.[5,8,9-11] Among the anatomical variations of the root canal, studies have shown that in spite of development of new systems and protocols for cleaning and shaping, isthmuses in root canals continue to be areas that are inaccessible to instruments, resulting in debris accumulation and the maintenance of necrotic pulp tissue and microorganisms inside the RCS, affecting 3D filling and, consequently, clinical outcomes.[10,11]

Bearing in mind the valuable contributions of micro-CT images in terms of resolution and reduced artifacts, several studies have assessed the accuracy of CBCT images for anatomical assessment, evaluation of biomechanical preparation, and RCS filling. This has led to a deeper understanding of the potential, optimized use, and limitations of CBCT, allowing this modality to be used in a manner that facilitates diagnosis and endodontic planning.[6,12-15]

However, some aspects regarding the diagnostic performance of CBCT during endodontic treatment remain unclear. Furthermore, due to the varying technical specifications of different CBCT devices, the consistency in diagnostic performance between CBCT systems and the effects of these specifications remains unclear.

The purpose of this study was to evaluate the performance of CBCT for the diagnosis and classification of isthmuses, and for assessing the cleaning, shaping, and filling of mesial roots of mandibular molars with isthmuses, using CBCT scanners with different technical specifications (tube current, tube voltage, exposure time, FOV size, and voxel size) compared to micro-CT as the gold standard.

Materials and Methods

After Research Ethics Committee approval (CAAE no. 80666517.2.0000.5419), 80 extracted mandibular human molars were collected from the teeth biobank of the Faculty of Dentistry of Ribeirão Preto, with complete rhizogenesis and a healthy root structure. For a criterion-based sample selection, the teeth were initially scanned with a SkyScan 1173 device (SkyScan, Kontich, Belgium). After scanning, 14 teeth with mesial roots that had 2 independent canals and the presence of isthmuses, while being free of pulp nodules and internal and/or external resorption, were selected. Only teeth with a moderate angle of curvature (between 10° and 20°), as measured using ImageJ (National Institutes of Health, Bethesda, MD, USA), were selected.

For the purpose of rehydration, teeth were identified and individually inserted into plastic receptacles containing 1 mL of saline solution and stored at 37°C and 95% relative humidity for 72 hours.

Biomechanical preparation of root canals

The crowns of teeth were maintained in order to clinically replicate the position of insertion and movement of endodontic instruments within the root canals. Access surgery was performed with a spherical drill #3 and an Endo Z drill bit driven by a high-speed motor. Each mesial canal was irrigated with 1 mL of 2.5% sodium hypochlorite using a NaviTip 30-gauge needle (Ultradent Products Inc., South Jordan, UT, USA). The canals were explored with a precurved #10 stainless steel manual K-file (Dentsply Maillefer, Ballaigues, Switzerland) that was carefully introduced into the canal until its tip coincided with the apical foramen, confirming the patency of the canal. From this length, 0.5 mm was subtracted to establish the working length. Cervical preparation was performed with a ProTaper Gold SX (Dentsply, Maillefer, Ballaigues, Switzerland) in continuous rotation (300 rpm, 5.10 N-cm). The instrument was introduced once, in the direction of the long axis of the tooth, to a depth corresponding to one-third of the working length, for 15 s, allowing direct access to the canal. After this, the canal was irrigated, aspirated and constantly flooded with 1 mL of 2.5% sodium hypochlorite.

Patency was performed at the working length, using manual #15 and #20 endodontic files (Dentsply, Maillefer, Ballaigues, Switzerland). The canals were prepared using a sequence of ProTaper Gold instruments S1 and S2 (Dentsply, Maillefer, Ballaigues, Switzerland), with in-and-out movements against the walls of the root canal in continuous rotation, for 15 s. Then, ProTaper Gold F1, F2, and F3 files were used (Dentsply, Maillefer, Ballaigues, Switzerland), with continuous movements of insertion and removal within the root canal, for 15 s, until the working length was reached. The instruments were mechanically driven by an X-Smart Plus 6 : 1 contra-angle (Dentsply, Maillefer, Ballaigues, Switzerland) coupled to a handpiece adapted to an X-Smart Plus electric motor (Dentsply, Maillefer, Ballaigues, Switzerland). The canals were prepared following the recommendations of the manufacturer of the ProTaper Gold system, with pre-defined parameters of torque and velocity corresponding to each instrument.

During the entire preparation, at each instrument change, the root canal was irrigated, aspirated, and flooded with 1 mL of 2.5% sodium hypochlorite using a Navitip 30-gauge needle (Ultradent Products Inc., South Jordan, UT, USA) adapted to the disposable plastic syringe, totaling 5 mL of solution in each canal.

Post-instrumentation scanning

First, the specimens were wrapped in paraffin and moistened with saline solution to prevent dehydration and consequent formation of microcracks and then they were scanned using a SkyScan 1173 device (SkyScan, Kontich, Belgium). The acquisition parameters were adjusted to 130 kV, 61 μA, voxel size of 12 μm, 360° of rotation, rotation step of 0.4°, 4 frames per rotation step. A bronze filter with thickness of 0.25 mm was used. The total scan time was 1.5 hours per sample. After the scans, the specimens were again stored in an oven (37°C, 95% relative humidity).

The images were reconstructed using NRecon v1.6.6.0 software (Bruker, Kontich, Belgium). Ring artifact correction with a value of 15 (range: 0-20), beam hardening correction of 30% (range: 0-100%), and a smoothing setting of 3 (range: 0-10) was applied. Reconstructed axial sections were saved in 14-bit DICOM format.

In order to simulate hard and soft tissues, a dry human mandible covered with a soft tissue simulator (MixD) was prepared,[16] and subsequently, the teeth were positioned within an enlarged alveolus. Each specimen was scanned using the following CBCT devices: 1. 3D Accuitomo 170 (J. Morita, Kyoto, Japan) 2. NewTom 5G (QR Verona, Verona, Italy) and 3. NewTom VGi evo (QR Verona, Verona, Italy). High-resolution protocols were selected according to each machine: 3D Accuitomo 170 (ACC): 5 mA, 90 kV, FOV of 4 × 4 cm, voxel size of 0.08 mm, exposure time of 30.8 s; NewTom 5G (N5G): 4.41 mA, 110 kV, FOV of 4 × 4, voxel size of 0.1 mm, exposure time of 7.3 s; NewTom VGi evo (NEVO): 3 mA, 110 kV, FOV of 5 × 5, voxel size of 0.1 mm, exposure time of 7.3 s.

Root canal filling

Prior to filling, 17% EDTA was applied in the canals for 3 minutes, followed by final irrigation with 10 mL of 2.5% sodium hypochlorite. Subsequently, specimens were dried with capillary tip aspiration cannulas (Ultradent, South Jordan, UT, USA) followed by F3 absorbent paper cones (Dentsply, Maillefer, Ballaigues, Switzerland) up to the working length and filled by means of thermoplastic continuous wave compaction (System B, Analytic Technology, Redmond, WA, USA).

AH Plus root canal sealer (Dentsply, Konstanz, Germany) was handled according to the manufacturer's recommendations, and a gutta-percha cone previously filled with sealer was gradually introduced up to the working length. Excess filling material was removed from the root canal entrance with a preheated fine medium condenser (Buchanan Plugger .08 Taper, SymbonEndo, Glendora, CA, USA) coupled with a Denjoy heat generating device (Denjoy Dental Co. Ltda, Changsha, Hunan, China). Then, with the gutta-percha still in a plasticized state, vertical condensation of the cone inside the root canal was performed with a cold manual condenser number 2 (Hand Pluggers Buchanan, SybronEndo, Glendora, CA, USA) with light but firm pressure in the apical direction for 5 s. Then, a heated Fine condenser (Buchanan Plugger .06 Taper, SybronEndo, Glendora, CA, USA) was used to make a cut at 3 mm of the working length (down-packing), in order to maintain the filling in the apical third only.

For filling the cervical and middle thirds, AH Plus (Dentsply, Konstanz, Germany) was placed on the walls of the root canal with the aid of an endodontic manual file type K #25 (Dentsply, Maillefer, Ballaigues, Switzerland), followed by injection of plastic gutta-percha, and cold vertical condensation was performed with a #2 manual condenser (Hand Pluggers Buchanan, SybronEndo, Glendora, CA, USA).

Post-filling scan

After filling, the specimens were subjected to a post-filling micro-CT examination. Subsequently, the specimens were repositioned in the human mandible, respecting the

same initial and post-test positions, and were subjected to a post-filling CBCT examination using the same parameters as previously described in the initial acquisition.

Image processing

For registration of the images of the 3 experimental phases (initial, post-preparation, and post-filling), MeVisLab software (MeVis Medical Solutions AG, Bremen, Germany) was used, using micro-CT scans (initial, post-preparation and post-filling, respectively) as fixed images and CBCT scans as moving images.

First, a region of interest (ROI) was selected and saved in the DICOM/TIFF format. After ROI selection, automatic registration was performed using "MTMScaffoldStrain" (KU Leuven, Belgium), in order to allow subsequent quantitative and qualitative analysis.

Quantitative analysis

The analysis was performed with CTAn software v.1.11.4.2 (SkyScan, Kontich, Belgium) using the Individual Object Analysis (2D space) plug-in. The following 2D parameters were measured: perimeter, area (mm^2), roundness, major and minor diameters (mm), and radicular sections of axial sections, at 3 root levels (cervical, middle and apical), totaling 9 measurements for each specimen, and then averaging the parameters for the root canal as a whole.

Qualitative analysis

Sections were grouped into 2 phases (post-preparation [n = 14] and post-filling [n = 14]) and into thirds (cervical [n = 14], middle [n = 14], and apical [n = 14]) and arranged randomly in different slides in PowerPoint (Microsoft, Redmond WA, USA) for a subsequent blind evaluation. A random number generator (https://www.random.org/lists) was used to generate a random sequence of images. Thus, 42 images per device were evaluated considering the entire root canal. For isthmus evaluation, 7 images referring to the apical third were not evaluated because they did not present an isthmus, totaling 35 images evaluated per device.

The qualitative assessment was performed by 2 qualified endodontic observers with experience in micro-CT and CBCT image analysis using a personal computer with a screen resolution of 1920 × 1080 (Inspiron 15″ 7568, Dell Computadores do Brasil Ltda, Eldorado do Sul, RS, Brazil). The process of observer calibration consisted of evaluating 20% of the total images, randomly selected, with a kappa value of 0.91 for intra-examiner agreement and 0.92 for inter-examiner agreement. The observers performed the qualitative analysis in two sessions, at least 15 days apart, in a dark room free of ambient noise. The brightness and contrast of the images were optimized for visualization of the qualitative parameters. The morphology of the RCS was classified as reported by Vertucci (1984),[17] and the isthmus morphology was classified according to Hsu and Kim's classification (1997).[18] The scores used during the root canal evaluations are detailed in Table 1. For the evaluation of the post-instrumentation images, the presence or absence of debris in the root canal and in the isthmus area was analyzed, and so was the presence of perforation (Fig. 1A). For the post-filling images, the presence or absence of root canal filling defects, the filling quality in the isthmus areas, and the presence or absence of perforation were analyzed (Fig. 1B). The examiners also evaluated their ability to perform a diagnosis on 80 randomly selected axial sec-

Table 1. Scores used to evaluate the presence of debris, root perforation and the filling ability in the root canals and isthmus area

Debris in root canals	1 - Absent 2 - Present 3 - Image does not permit adequate diagnosis
Debris in isthmus area	1 - Absence of debris 2 - Isthmus partially filled with debris 3 - Isthmus completely filled with debris 4 - Image does not permit adequate diagnosis of the presence of debris 5 - Isthmus not detectable
Root canal perforation	1 - Absent 2 - Present 3 - Image does not permit adequate diagnosis
Root canal system filling	1 - Absence of filling defects* 2 - Presence of defects* of filling material 3 - Presence of defects* at the filling/dentin interface 4 - Presence of defects* of the filling material and at the dentin interface 5 - Image does not permit adequate diagnosis
Isthmus area filling	1 - Absent filling material 2 - Isthmus partially occupied by filling material 3 - Isthmus completely occupied by filling material 4 - Image does not permit adequate diagnosis of filling material 5 - Isthmus not detectable
Root canal perforation	1 - Absent 2 - Present 3 - Image does not permit adequate diagnosis

*Voids in the filling material and misalignment at the filling/dentin wall interface.

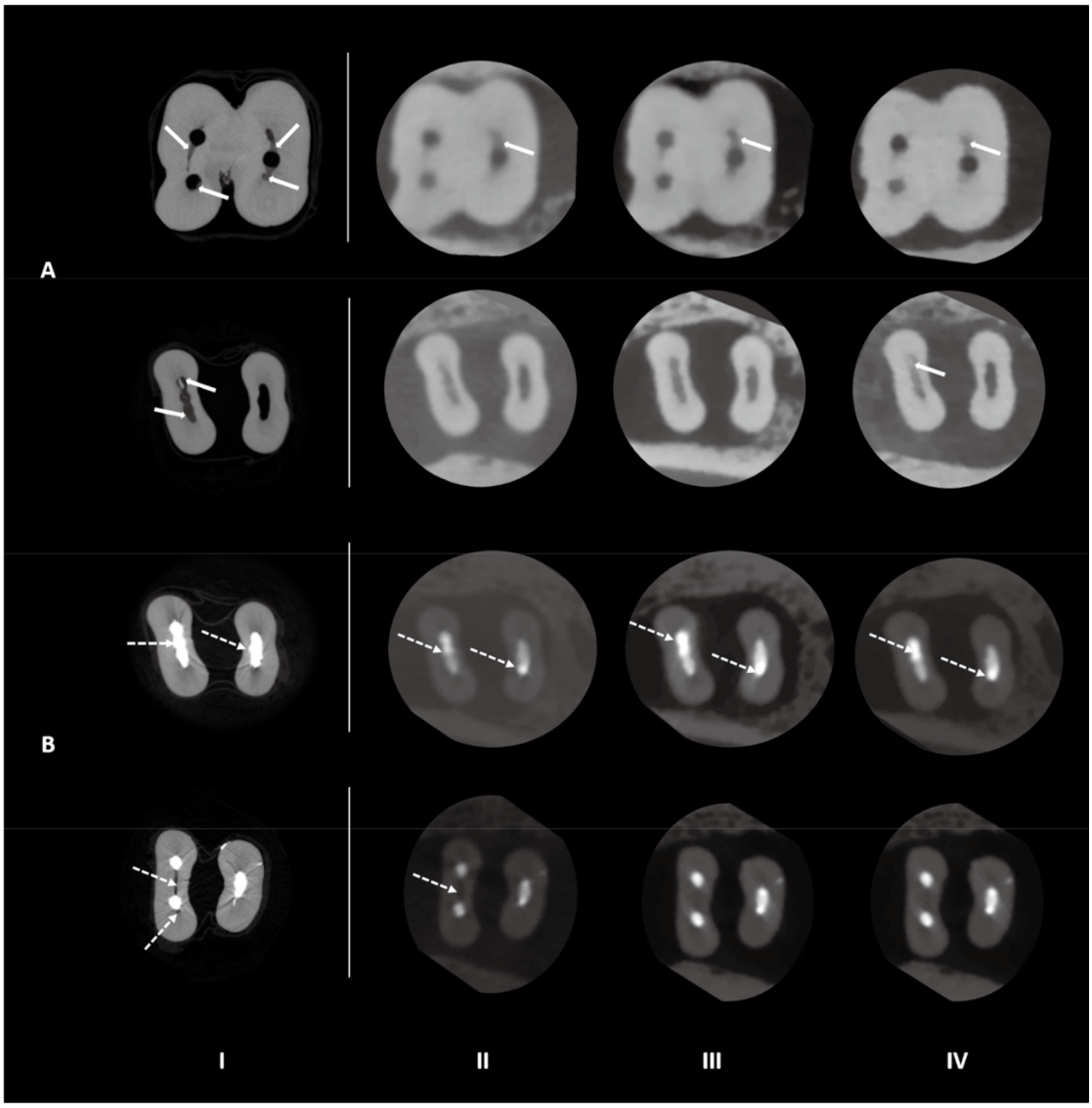

Fig. 1. A. Continuous white arrows indicate the presence of debris in the isthmus area. B. Dotted white arrows show the quality of the isthmus and root canal filling. I: micro-CT, II: 3D Accuitomo 170, III: NewTom 5G, IV: NewTom VGi evo.

tions at different phases of endodontic treatment. For each image, the examiners graded the confidence level of their response with respect to diagnostic ability on a scale from 0 to 6, where 0 was "not confident" and 6 was "extremely confident."

Statistical analysis

Quantitative data for area, perimeter, roundness, major diameter and minor diameters were initially subjected to tests of normality (Shapiro-Wilk) and homogeneity of variance (Levene test). After the normality and homogeneity of the sample distribution were verified, the data were subjected to 1-way analysis of variance to evaluate the influence of the scanner (micro-CT, ACC, N5G, and NEVO) and the Tukey test for multiple comparisons between groups. The agreement between the quantitative data between the different CBCT and micro-CT devices was quantified in terms of the intraclass correlation coefficient (ICC). The relationship between the quantitative data obtained by micro-CT and each of the 3 CBCT devices was determined by simple linear regression.

The qualitative data were presented as frequency distribution and percentage observed, and analyzed for agreement between the different devices using the kappa coefficient. All analyses were performed in SPSS version 15.0 (SPSS, Inc., Chicago, IL, USA) with a 0.05 significance level.

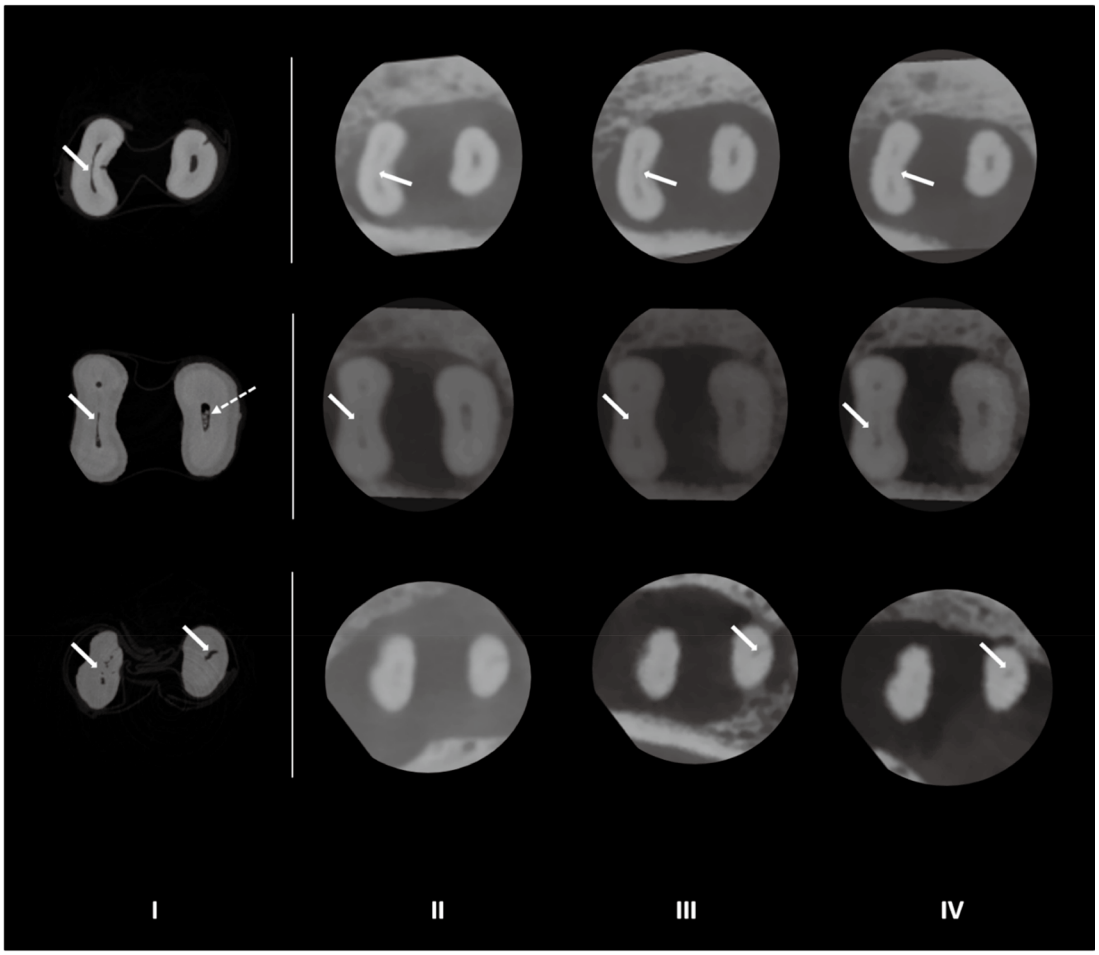

Fig. 2. Continuous white arrows indicate the presence of the isthmus area in root canals of mandibular molars, and dotted white arrows indicate the presence of debris. I: micro-CT, II: 3D Accuitomo 170, III: NewTom 5G, IV: NewTom VGi evo.

Results

Analysis of the RCS

Isthmus types IV and V were the most frequently reported for all devices evaluated (Fig. 2). For type I (absence of an isthmus), CBCT showed a higher frequency (20%-22.5%) than micro-CT (5%). In contrast, higher frequencies of types II (20%) and III (10%) were observed in the images captured with micro-CT (Table 2, Fig. 2).

No significant differences between the CBCT devices were found for the area ($P=0.59$), roundness ($P=0.35$) and minor diameter ($P=0.10$). For the perimeter, micro-CT showed higher values than CBCT ($P<0.05$). For the major diameter, micro-CT showed higher values than ACC and NEVO ($P<0.05$), whereas the N5G device showed major diameter values similar to those of micro-CT, ACC, and NEVO ($P>0.05$) (Table 3).

The simple linear regression models, presented in Figure 3, showed significant associations between area, perimeter, roundness, and major diameter and the imaging modality (micro-CT and the various CBCT devices) ($P<0.01$).

Analysis after biomechanical preparation of the root canal

Table 4 and Figure 4 show the distribution of findings regarding the presence of debris in the root canal and isthmus area. In the evaluation by micro-CT, debris was observed in 40.7% of the canals. Most of the CBCT images did not permit a diagnosis, and among the images that did allow a diagnosis, the majority did not show the presence of debris in the root canal. The kappa test indicated moderate agreement between micro-CT and the ACC and NEVO devices ($\kappa=0.45$ and $\kappa=0.46$, respectively). Among the CBCT devices, there was no agreement between N5G and ACC ($\kappa=0.12$), and N5G and NEVO ($\kappa=0.06$), but substantial agreement between ACC and NEVO ($\kappa=0.70$).

Table 2. Classification of the root canal system morphology of the mesial root of mandibular molars [n (%)] according to Vertucci and the type of isthmus according to Hsu and Kim, for the different devices evaluated

Devices	Vertucci's morphology							
	I	II	III	IV	V	VII	II-I-II-I	I-II-I-II-I
Micro-CT	5 (35.8)	–	2 (14.3)	2 (14.3)	3 (21.4)	–	1 (7.1)	1 (7.1)
3D Accuitomo 170	3 (21.4)	1 (7.1)	3 (21.4)	2 (14.3)	2 (14.3)	2 (14.3)	1 (7.1)	–
NewTom 5G	3 (21.4)	1 (7.1)	3 (21.4)	2 (14.3)	2 (14.3)	2 (14.3)	1 (7.1)	–
NewTom VGi evo	3 (21.4)	1 (7.1)	3 (21.4)	2 (14.3)	2 (14.3)	1 (7.1)	1 (7.1)	1 (7.1)
Devices	Isthmus morphology							
	I	II	III	IV	V			
Micro-CT	2 (5.0)	8 (20.0)	4 (10.0)	12 (30.0)	14 (35.0)			
3D Accuitomo 170	8 (20.0)	2 (5.0)	–	13 (32.5)	17 (42.5)			
NewTom 5G	9 (22.5)	5 (12.5)	1 (2.5)	10 (25.0)	15 (37.5)			
NewTom VGi evo	9 (22.5)	3 (7.5)	–	14 (35.0)	14 (35.0)			

Table 3. Values of area (mm^2), perimeter (mm), roundness (mm), and the major and minor diameters (mm) before and after root canal biomechanical preparation and after root canal filling

	Devices	Area	Perimeter	Roundness	Major diameter	Minor diameter
Root canal before biomechanical preparation	Micro-CT	0.51 ± 0.46^{A}	3.68 ± 2.14^{A}	0.41 ± 0.24^{A}	1.44 ± 0.94^{A}	0.47 ± 0.20^{A}
	3D Accuitomo 170	0.43 ± 0.54^{A}	2.40 ± 2.27^{B}	0.36 ± 0.29^{A}	0.95 ± 0.97^{B}	0.38 ± 0.30^{A}
	NewTom 5G	0.45 ± 0.50^{A}	2.57 ± 2.13^{B}	0.37 ± 0.26^{A}	1.01 ± 0.90^{AB}	0.43 ± 0.28^{A}
	NewTom VGi evo	0.39 ± 0.52^{A}	2.16 ± 2.19^{B}	0.31 ± 0.26^{A}	0.85 ± 0.02^{B}	0.35 ± 0.30^{A}
	P value	0.59	0.01	0.35	0.05	0.1
Root canal after biomechanical preparation	Micro-CT	0.50 ± 0.37^{A}	2.85 ± 1.53^{A}	0.72 ± 0.24^{A}	0.94 ± 0.59^{A}	0.67 ± 0.23^{A}
	3D Accuitomo 170	0.51 ± 0.43^{A}	2.77 ± 2.64^{A}	0.66 ± 0.25^{A}	0.92 ± 0.63^{A}	0.58 ± 0.28^{A}
	NewTom 5G	0.47 ± 0.39^{A}	2.52 ± 1.43^{A}	0.71 ± 0.21^{A}	0.87 ± 0.59^{A}	0.63 ± 0.25^{A}
	NewTom VGi evo	0.49 ± 0.42^{A}	2.57 ± 1.52^{A}	0.67 ± 0.22^{A}	0.89 ± 0.60^{A}	0.63 ± 0.28^{A}
	P value	0.92	0.51	0.28	0.90	0.19
After root canal filling	Micro-CT	0.64 ± 0.50^{A}	3.27 ± 1.65^{A}	0.70 ± 0.20^{A}	1.10 ± 0.66^{A}	0.77 ± 0.23^{A}
	3D Accuitomo 170	0.45 ± 0.48^{AB}	2.40 ± 1.62^{B}	0.67 ± 0.20^{A}	0.90 ± 0.68^{AB}	0.57 ± 0.27^{B}
	NewTom 5G	0.38 ± 0.54^{B}	2.10 ± 1.83^{B}	0.57 ± 0.24^{B}	0.75 ± 0.71^{B}	0.46 ± 0.32^{B}
	NewTom VGi evo	0.42 ± 0.45^{B}	2.23 ± 1.63^{B}	0.64 ± 0.24^{AB}	0.80 ± 0.67^{B}	0.52 ± 0.27^{B}
	P value	0.009	<0.001	0.009	0.12	<0.001

Different letters indicate statistically significant differences according to the Tukey test ($P<0.05$) for the different parameters evaluated.

The presence of debris was observed in 91.4% of the isthmuses when evaluated by micro-CT. For CBCT, 37.1% of the images from NEVO, 42.9% from N5G, and 45.7% from ACC did not permit an adequate diagnosis of the presence of debris (Table 4).

Kappa analysis did not show agreement in the classification of the presence of debris in the root canal and isthmus after biomechanical preparation between the micro-CT and the CBCT devices ($0.05<\kappa<0.12$). Among the CBCT devices, moderate agreement was observed between N5G and ACC ($\kappa=0.45$) and between N5G and NEVO ($\kappa=0.42$), while substantial agreement was found between ACC and NEVO ($\kappa=0.65$). Root canal perforation was detected in 0% of the micro-CT images, whereas the presence of perforation was reported in around 2.4%-4.8% of the images captured with the CBCT devices (Table 5).

The quantitative analysis of area, perimeter, roundness, and the major and minor diameters after biomechanical

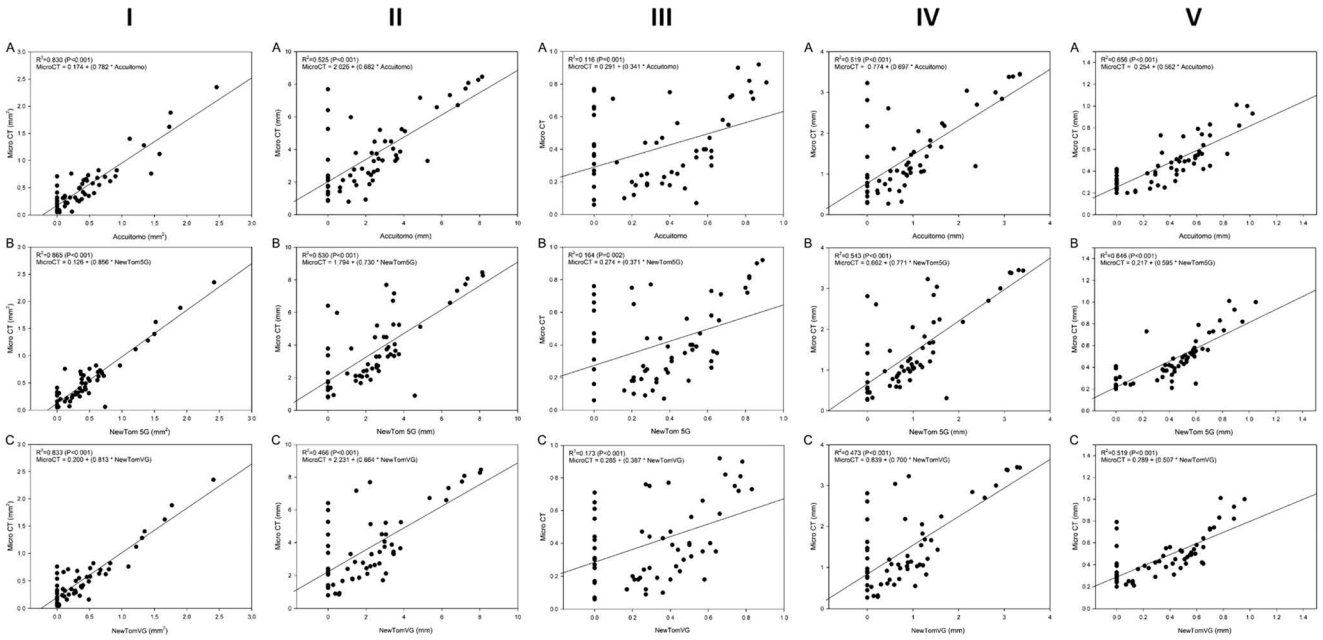

Fig. 3. Linear regression models for images obtained before biomechanical root canal preparation. A. Linear regression values between micro-CT and 3D Accuitomo 170. B. Linear regression values between micro-CT and NewTom 5G. C. Linear regression values between micro-CT and NewTom VGi evo. I: area, II: perimeter, III: roundness, IV: major diameter, V: minor diameter.

Table 4. Classification of the presence of debris in the root canal and in the isthmus area [n (%)] after biomechanical preparation

Devices	Debris in the root canal				
	Absent	Present	Indeterminate		
Micro-CT	24 (57.1)	17 (40.5)	1 (2.4)		
3D Accuitomo 170	6 (14.3)	–	36 (85.7)		
NewTom 5G	13 (31)	2 (4.8)	27 (64.3)		
NewTom VGi evo	18 (42.9)	2 (4.8)	22 (52.4)		
Devices	**Debris in the isthmus**				
	Absent	Partially filled	Completely filled	Indeterminate	Not detectable
Micro-CT	3 (8.6)	7 (20.0)	25 (71.4)	–	–
3D Accuitomo 170	2 (5.7)	–	2 (5.7)	16 (45.7)	15 (42.9)
NewTom 5G	1 (2.9)	–	5 (14.3)	15 (42.9)	14 (40.0)
NewTom VGi evo	3 (8.6)	1 (2.9)	4 (11.4)	13 (37.1)	14 (40.0)

preparation is presented in Table 3. There were no significant differences among micro-CT and the CBCT devices (Table 3).

For area, perimeter, roundness, and the major and minor diameters, the CBCT devices showed satisfactory reproducibility when compared to micro-CT ($0.60 < ICC < 0.73$). Among the CBCT devices, excellent reproducibility was observed for area, perimeter, and the major and minor diameters ($ICC \geq 0.75$) and satisfactory reproducibility for roundness ($0.69 < ICC < 0.73$). The simple linear regression models are shown in Figure 5. For the perimeter and major diameter, the linear regression models showed high regression coefficients between micro-CT and N5G (0.80 and 0.86, respectively), whereas the linear regression models between micro-CT and ACC and between micro-CT and NEVO yielded lower regression coefficient values (0.57 and 0.7, respectively) (Fig. 3). For roundness (0.36-0.54) and minor diameter (0.65-0.73) a higher regression co-

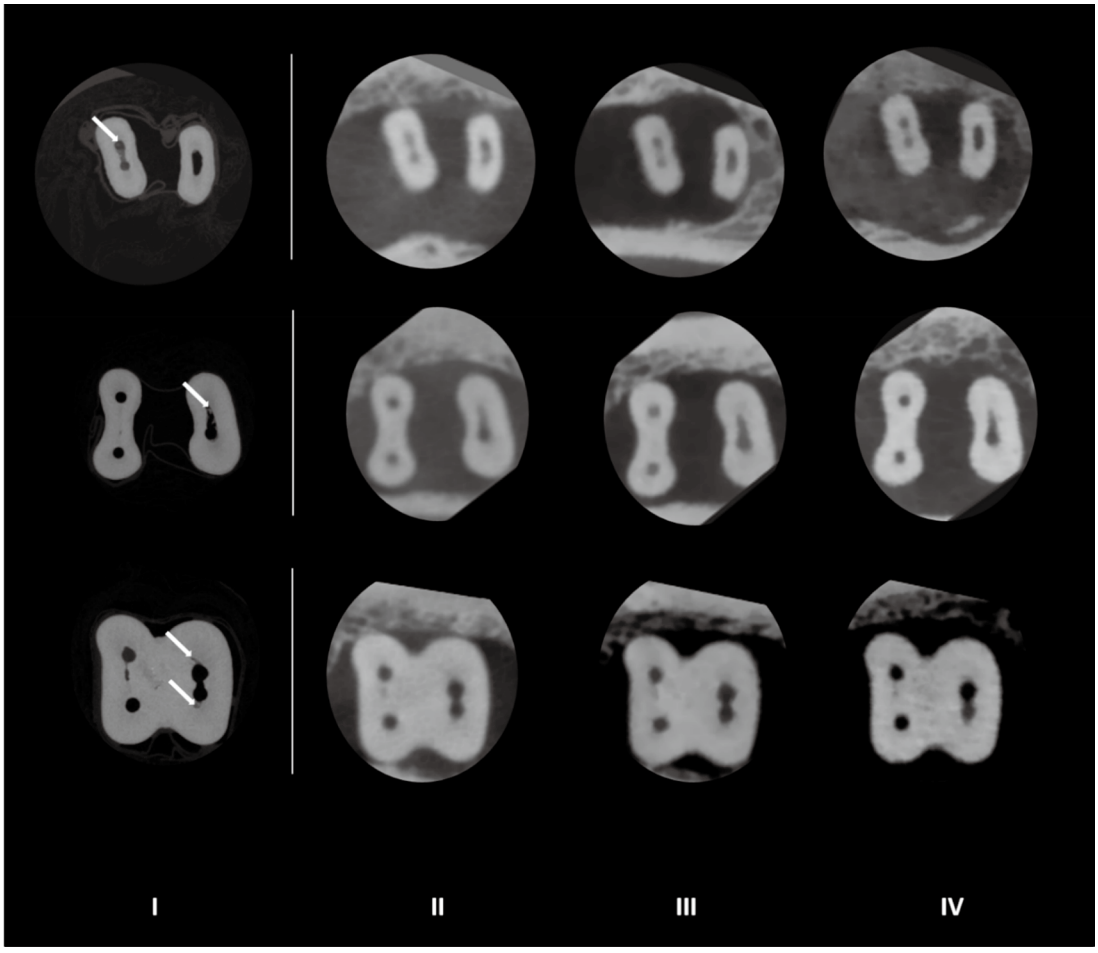

Fig. 4. White arrows indicate the presence of debris in the isthmus area in root canals of mandibular molars diagnosed with better visualization on micro-CT. I: micro-CT, II: 3D Accuitomo 170, III: NewTom 5G, IV: NewTom VGi evo.

Table 5. Classification of the presence of root perforation [n (%)] after biomechanical preparation and after root canal filling

	Devices	Absent	Present	Indeterminate
Root perforation after biomechanical preparation	Micro-CT	42 (100.0)	–	–
	3D Accuitomo 170	41 (97.6)	1 (2.4)	–
	NewTom 5G	40 (95.2)	2 (4.8)	–
	NewTom VGi evo	41 (97.6)	1 (2.4)	–
Root perforation after root canal filling	Micro-CT	41 (97.6)	1 (2.4)	–
	3D Accuitomo 170	36 (85.7)	2 (4.8)	4 (9.5)
	NewTom 5G	41 (97.6)	1 (2.4)	–
	NewTom VGi evo	41 (97.6)	1 (2.4)	–

efficient was observed for N5G ($\beta = 0.82$) than for ACC ($\beta = 0.63$) and NEVO ($\beta = 0.64$) (Fig. 5).

Analysis after root canal filling

The results of root canal and isthmus filling quality and root canal perforation after filling are presented in Figure 6 and Tables 5 and 6. Micro-CT showed an absence of voids in 69% of the images (Table 6, Fig. 6), whereas the ACC device did not allow diagnosis in 88.1% of the images, followed by 45.2% for the N5G device and 14.3% for the NEVO device (Table 6, Fig. 6). Kappa analysis indicated an absence of agreement among all the devices evaluated ($0.01 < \kappa < 0.16$).

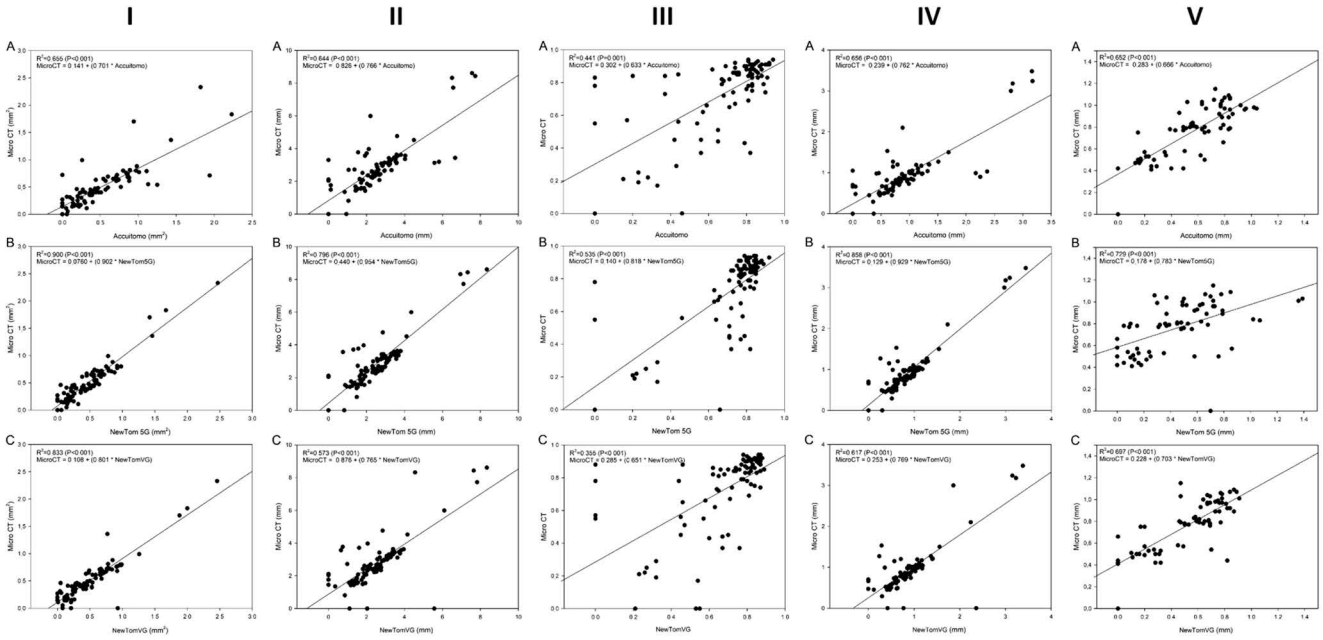

Fig. 5. Linear regression models for images obtained after biomechanical root canal preparation. A. Linear regression values between micro-CT and 3D Accuitomo 170. B. Linear regression values between micro-CT and NewTom 5G. C. Linear regression values between micro-CT and NewTom VGi evo. I: area, II: perimeter, III: roundness, IV: major diameter, V: minor diameter.

Table 6. Classification of the quality of filling [n (%)] in the root canals and in the isthmus area

	Devices	1	2	3	4	5
Root canal filling quality*	Micro-CT	29 (69.0)	–	9 (21.4)	4 (9.5)	–
	3D Accuitomo 170	4 (9.5)	–	–	1 (2.5)	37 (88.1)
	NewTom 5G	21 (50.0)	–	–	2 (4.8)	19 (45.2)
	NewTom VGi evo	33 (78.6)	–	–	3 (7.1)	6 (14.3)
Isthmus filling quality**	Micro-CT	17 (48.6)	9 (25.7)	9 (25.7)	–	–
	3D Accuitomo 170	1 (2.9)	1 (2.9)	9 (25.7)	8 (22.8)	16 (45.7)
	NewTom 5G	–	3 (8.6)	10 (28.6)	6 (17.1)	16 (45.7)
	NewTom VGi evo	1 (2.9)	3 (8.6)	10 (28.6)	4 (11.4)	17 (48.5)

*Scores for the classification of root canal filling quality. 1: absence of defects, 2: presence of defects in the filling material, 3: presence of defects at the filling/dentin wall interface, 4: presence of defects in the filling material and the dentin interface, 5: image does not allow adequate diagnosis. **Scores for classification of filling quality in the isthmus. 1: filling material absent, 2: isthmus partially filled with filling material, 3: isthmus completely filled with filling material, 4: image does not allow adequate diagnosis of filling material, and 5: not detectable.

For CBCT, 22.8% of the images captured by ACC, 17.1% of those obtained by N5G, and 11.4% of those captured by NEVO did not allow an adequate diagnosis of the presence of filling material in the isthmus area, and for 45.7% to 48.5% of the images evaluated, it was not possible to detect the presence of an isthmus (Table 6). Perforation after root canal filling was detected in 1 tooth for micro-CT, N5G, and NEVO, and in 2 teeth for ACC (Table 5).

For area, perimeter, and the major and minor diameters, significant differences were observed between the CBCT devices evaluated (Table 3). For perimeter and the minor diameter, the micro-CT showed higher values than the CBCT devices ($P<0.05$). For area and the major diameter, micro-CT showed higher values than N5G and NEVO ($P<0.05$), whereas the ACC device showed values similar to those of micro-CT, N5G, and NEVO ($P>0.05$). For roundness, micro-CT and ACC showed the highest values, without a statistically significant difference between them ($P>0.05$). The lowest values were observed for the N5G device ($P<0.05$), whereas the NEVO device showed intermediate values, similar to those of micro-CT, ACC, and N5G ($P>0.05$) (Table 3).

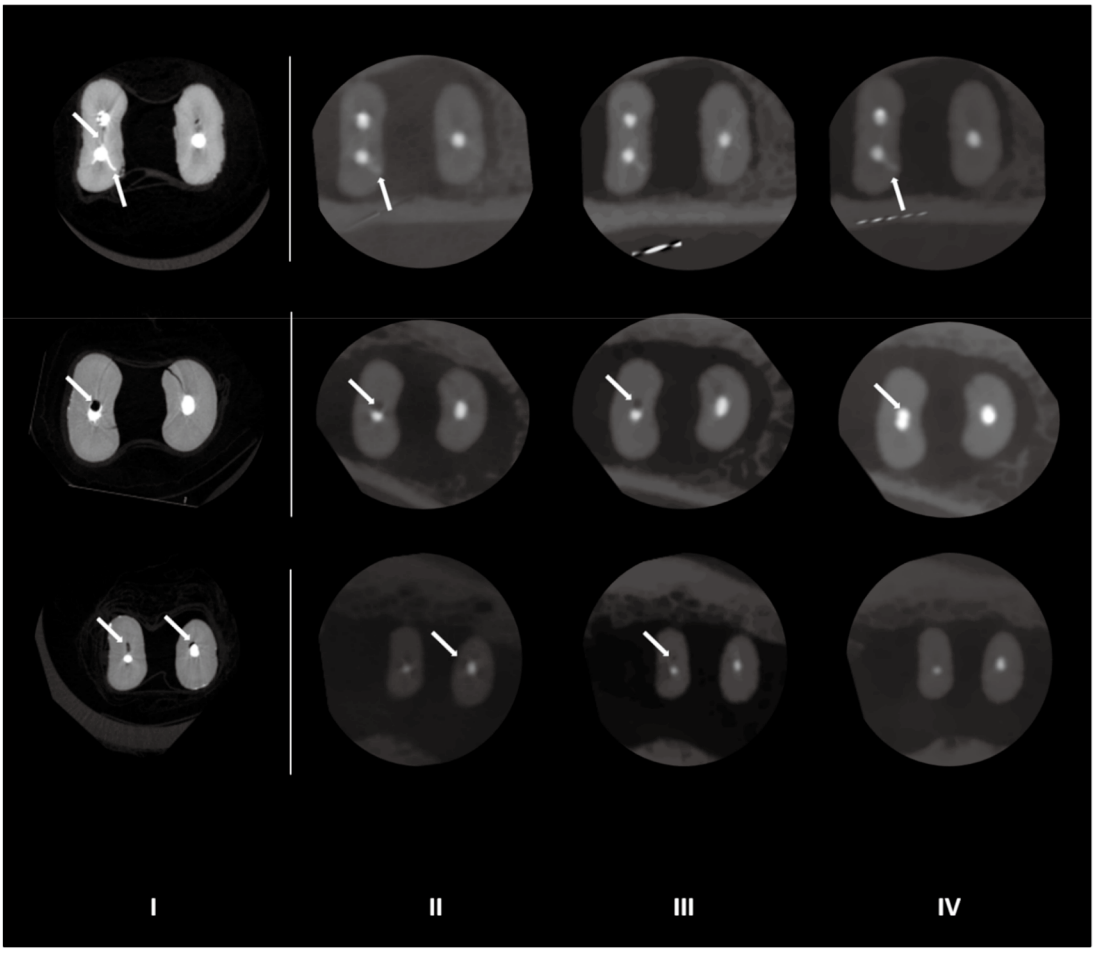

Fig. 6. White arrows showing the quality of the isthmus and root canal filling. It is possible to detect in micro-CT images (I) the presence of filling material in the isthmus area, the presence of gaps and voids, as well as lateral and accessory filled canals, which are not seen in the CBCT images and could hinder the endodontic diagnosis. II: 3D Accuitomo 170, III: NewTom 5G, III: NewTom VGi evo.

Simple linear regression models, presented in Figure 7, showed significant associations between area, perimeter, roundness, and the major and minor diameters for the data evaluated by micro-CT and CBCT devices ($P < 0.05$).

Discussion

CBCT is an interdisciplinary clinical imaging resource that has been widely used in the diagnosis, planning, treatment, and follow-up processes involving the application of radiology in the endodontics field, mainly in the areas of anatomical challenges, fractures, perforations, internal or external resorption, and evaluations of the quality or failure of treatment.[1,5,9,16,19,20] However, it is noteworthy that each CBCT machine has different performance in terms of the radiation dose, technical image quality, and diagnostic image quality, which determines its applicability for the different steps of root canal treatment.[5,9,20]

In this context, the present study evaluated how the morphological configuration of the RCS of mandibular molars with an isthmus impacted the diagnosis, cleaning, shaping, and filling of the root canals after evaluating the images captured by different CBCT devices, acquired with different technical specifications, using the image data obtained from micro-CT as reference standard, by means of qualitative and quantitative analyses.

The RCS configuration was assessed according to the morphological classification of Vertucci[17] and the classification of isthmuses of Hsu and Kim.[18] Regarding the classification of root canals, Vertucci[17] described 8 different morphological types, and in the sample of the present study, it was possible to observe the presence of types I, III, IV, and V in images captured by all the devices evaluated (CBCT and micro-CT). The qualitative analysis of the images detected a higher prevalence of types IV and V among the 5 types of isthmus described by Hsu and Kim[18] both in micro-

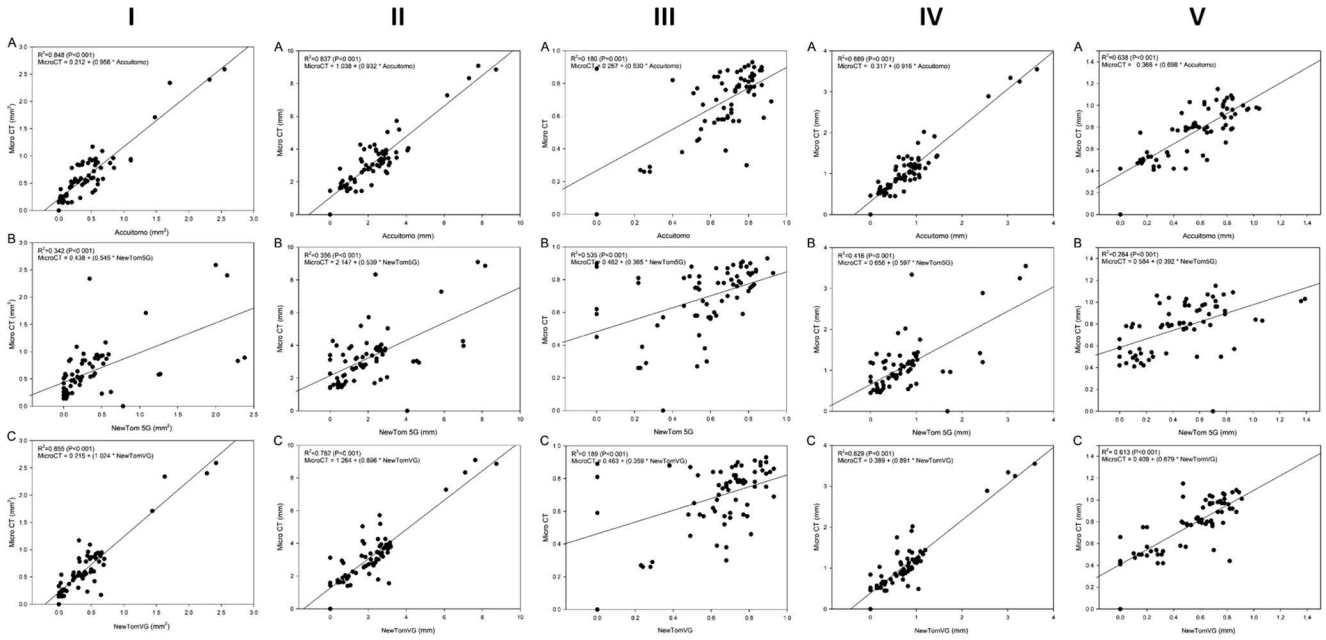

Fig. 7. Linear regression models for images obtained after root canal filling. A. Linear regression values between micro-CT and 3D Accuitomo 170. B. Linear regression values between micro-CT and NewTom 5G. C. Linear regression values between micro-CT and NewTom VGi evo. I: area, II: perimeter, III: roundness, IV: major diameter, V: minor diameter.

CT and CBCT images. However, it was more difficult to classify isthmus types II and III correctly on the CBCT images. Regardless, it is worth noting that despite the difficulty of classifying the type of isthmus, the possibility of diagnosing its presence by CBCT allows the clinician to consider the isthmus while planning endodontic treatment.[20]

After biomechanical preparation, approximately 40% of the CBCT images did not allow the diagnosis of the presence of an isthmus; this was possibly directly related to the accumulation of debris in these challenging anatomical areas, since debris and dentin have similar densities. These data corroborated the results obtained in the morphological evaluation of the RCS, in which it was also difficult to diagnose the presence of isthmuses in 20% to 22.5% of CBCT scans.[20]

It was possible to detect the presence of debris in around 40.5% of RCSs and in 91.4% of isthmus areas using micro-CT. In the majority of CBCT images, it was not possible to adequately diagnose debris within the root canals (52.4% to 85.7%). The limited ability to visualize isthmuses and debris is likely caused primarily by each device's limits of spatial resolution compared with micro-CT.[3,9,16,2021,22] In addition, for small low-contrast structures in particular, the contrast-to-noise ratio of the image plays a role. The reasons for qualitative differences between CBCT machines are difficult to pinpoint, although the image quality is affected by a multitude of factors, such as focal spot size, detector specifications, exposure parameters, and reconstruction settings.[20-22]

Micro-CT showed root perforations in 0% of the images evaluated after root preparation. However, images captured by CBCTs showed root perforations in 2.4% and 4.8% of the images analyzed, due to overestimating the root canal boundaries and underestimating the dentin thickness after biomechanical preparation. Limited sharpness and contrast of the root and root canals were also observed in the present study in the quantitative analysis of the original anatomy of the root canal (perimeter and major and minor diameters).

Two-dimensional quantitative analysis showed no statistically significant differences in area, perimeter, roundness, and the major and minor diameters between the different CBCT devices and micro-CT, with excellent and satisfactory agreement between CBCT and micro-CT. It is worth mentioning that biomechanical preparation improved the visualization of the RCS by CBCT, since the canals became wider, sharper and better delineated, explaining the qualitative and quantitative results obtained.[20]

In the present study, filling quality was evaluated according to the presence and absence of voids and their locations. When filling failure was located at the filling/dentin wall interface, as was present in 21.4% of the images

captured by micro-CT, none of the CBCT devices were able to depict it. This was probably due to the formation of artifacts in these images, especially in the delimitation of objects of high density, caused by the presence of dense filling material, the relatively low exposure used in CBCT versus micro-CT, along with the limited sharpness and contrast, which are factors inherent to all the CBCT devices that were evaluated.[3,9,20,23-25]

After filling, 47.1% to 50% of the CBCT images did not allow detection of the isthmus. However, when the isthmus was completely occupied by filling material, it was possible to diagnose it in 26.5% of the images captured by micro-CT and ACC and in 29.4% of the images captured by N5G and NEVO, showing uniform agreement of results between micro-CT and the CBCT devices evaluated. The CBCT images showed partially filled isthmuses in 2.9% of scans for the ACC device and 8.8% for the N5G and NEVO devices, versus 26.5% for micro-CT. However, the quantitative analysis of the area, perimeter and the major and minor diameters demonstrated excellent agreement between CBCT and micro-CT. The roundness values presented satisfactory agreement between the CBCT devices and micro-CT, demonstrating the limitation of the CBCT devices in reproducing the delimitation of filling material with sharpness and accuracy, probably due to artifact generation as previously observed in the qualitative evaluation.[20] Thus, the clinical use of CBCT to diagnose and evaluate the quality of the RCS filling should be viewed with caution, since the formation of artifacts resulting from high-density materials can lead to the formulation of false diagnoses, as well as masking structures and/or pathoses.[20,25-29]

Considering that the isthmus is a challenging anatomical area that has a direct impact on the success of endodontic treatment, it was observed in the present study that CBCT devices have sufficient sensitivity and accuracy in the detection of isthmuses; however, they did not allow their classification after biomechanical preparation and root canal filling. In addition, blooming and dark streak artifacts after endodontic filling may hamper the diagnosis and mask filling voids and specific pathologies in the neighborhood of the RCS and isthmus.

Conflicts of Interest: None

References

1. Estrela C, Rabelo LE, de Souza JB, Alencar AH, Estrela CR, Sousa Neto MD, et al. Frequency of root canal isthmi in human permanent teeth determined by cone-beam computed tomography. J Endod 2015; 41: 1535-9.
2. Patel K, Mannocci F, Patel S. The assessment and management of external cervical resorption with periapical radiographs and cone-beam computed tomography: a clinical study. J Endod 2016; 42: 1435-40.
3. Beacham JT, Geist JR, Yu Q, Himel VT, Sabey KA. Accuracy of cone-beam computed tomographic image interpretation by endodontists and endodontic residents. J Endod 2018; 44: 571-5.
4. Martins JN, Ordinola-Zapata R, Marques D, Francisco H, Caramês J. Differences in root canal system configuration in human permanent teeth within different age groups. Int Endod J 2018; 51: 931-41.
5. Patel S, Brown J, Pimentel T, Kelly RD, Abella F, Durack C. Cone beam computed tomography in Endodontics - a review of the literature. Int Endod J 2019; 52: 1138-52.
6. Mazzi-Chaves JF, de Faria Vasconcelos K, Pauwels R, Jacobs R, Sousa-Neto MD. Cone-beam computed tomographic-based assessment of filled c-shaped canals: artifact expression of cone-beam computed tomography as opposed to micro-computed tomography and nano-computed tomography. J Endod 2020; 46: 1702-11.
7. Sousa-Neto MD, Silva-Sousa YC, Mazzi-Chaves JF, Carvalho KK, Barbosa AF, Versiani MA, et al. Root canal preparation using micro-computed tomography analysis: a literature review. Braz Oral Res 2018; 32 (suppl 1): e66.
8. Camargo RV, Mazzi-Chaves JF, Leoni GB, Vasconcelos KF, Lamira A, Jacobs R, et al. Quantitative assessment of 2-dimensional parameters in tomographic images by using different segmentation methods. J Endod 2020; 46: 694-9.
9. Patel S, Brown J, Semper M, Abella F, Mannocci F. European Society of Endodontology position statement: Use of cone beam computed tomography in Endodontics: European Society of Endodontology (ESE) developed by. Int Endod J 2019; 52: 1675-8.
10. Bechara B, Alex Mcmahan C, Moore WS, Noujeim M, Teixeira FB, Geha H. Cone beam CT scans with and without artefact reduction in root fracture detection of endodontically treated teeth. Dentomaxillofac Radiol 2013; 42: 20120245.
11. Keleş A, Keskin C. A micro-computed tomographic study of band-shaped root canal isthmuses, having their floor in the apical third of mesial roots of mandibular first molars. Int Endod J 2018; 51: 240-6.
12. Malentacca A, Lajolo C. A new technique to make transparent teeth without decalcifying: description of the methodology and micro-hardness assessment. Ann Anat 2015; 197: 11-5.
13. Maret D, Peters OA, Galibourg A, Dumoncel J, Esclassan R, Kahn JL, et al. Comparison of the accuracy of 3-dimensional cone-beam computed tomography and micro-computed tomography reconstructions by using different voxel sizes. J Endod 2014; 40: 1321-6.
14. Shaheen E, Khalil W, Ezeldeen M, Van de Casteele E, Sun Y, Politis C, et al. Accuracy of segmentation of tooth structures using 3 different CBCT machines. Oral Surg Oral Med Oral Pathol Oral Radiol 2017; 123: 123-8.
15. Ordinola-Zapata R, Bramante CM, Versiani MA, Moldauer BI, Topham G, Gutmann JL, et al. Comparative accuracy of the clearing technique, CBCT and micro-CT methods in studying the mesial root canal configuration of mandibular first molars.

Int Endod J 2017; 50: 90-6.
16. Oenning AC, Salmon B, Vasconcelos KF, Pinheiro Nicolielo LF, Lambrichts I, Sanderink G, et al. DIMITRA paediatric skull phantoms: development of age-specific paediatric models for dentomaxillofacial radiology research. Dentomaxillofac Radiol 2018; 47: 20170285.
17. Vertucci FJ. Root canal anatomy of the human permanent teeth. Oral Surg Oral Med Oral Pathol 1984; 58: 589-99.
18. Hsu YY, Kim S. The resected root surface. The issue of canal isthmuses. Dent Clin North Am 1997; 41: 529-40.
19. Jacobs R. Dental cone beam CT and its justified use in oral health care. JBR-BTR 2011; 94: 254-65.
20. Rodrigues CT, Jacobs R, Vasconcelos KF, Lambrechts P, Rubira-Bullen IR, Gaêta-Araujo H, et al. Influence of CBCT-based volumetric distortion and beam hardening artefacts on the assessment of root canal filling quality in isthmus-containing molars. Dentomaxillofac Radiol 2021; 50: 20200503.
21. Pauwels R, Beinsberger J, Collaert B, Theodorakou C, Rogers J, Walker A, et al. Effective dose range for dental cone beam computed tomography scanners. Eur J Radiol 2012; 81: 267-71.
22. Nemtoi A, Czink C, Haba D, Gahleitner A. Cone beam CT: a current overview of devices. Dentomaxillofac Radiol 2013; 42: 20120443.
23. Decurcio DA, Bueno MR, De Alencar AH, Porto OC, Azevedo BC, Estrela C. Effect of root canal filling materials on dimensions of cone-beam computed tomography images. J Appl Oral Sci 2012; 20: 260-7.
24. Mazzi-Chaves JF, Camargo RV, Borges AF, Silva RG, Pauwels R, Silva-Sousa YT, et al. Cone-beam computed tomography in endodontics - state of the art. Curr Oral Health Rep 2021; 8: 9-22.
25. Bechara B, McMahan CA, Nasseh I, Geha H, Hayek E, Khawam G, et al. Number of basis images effect on detection of root fractures in endodontically treated teeth using a cone beam computed tomography machine: an in vitro study. Oral Surg Oral Med Oral Pathol Oral Radiol 2013; 115: 676-81.
26. Vasconcelos KF, Nicolielo LF, Nascimento MC, Haiter-Neto F, Bóscolo FN, Van Dessel J, et al. Artefact expression associated with several cone-beam computed tomographic machines when imaging root filled teeth. Int Endod J 2015; 48: 994-1000.
27. Brito-Júnior M, Santos LA, Faria-e-Silva AL, Pereira RD, Sousa-Neto MD. Ex vivo evaluation of artifacts mimicking fracture lines on cone-beam computed tomography produced by different root canal sealers. Int Endod J 2014; 47: 26-31.
28. Celikten B, Jacobs R, deFaria Vasconcelos K, Huang Y, Nicolielo LF, Orhan K. Assessment of volumetric distortion artifact in filled root canals using different cone-beam computed tomographic devices. J Endod 2017; 43: 1517-21.
29. Codari M, de Faria Vasconcelos K, Ferreira Pinheiro Nicolielo L, Haiter Neto F, Jacobs R. Quantitative evaluation of metal artifacts using different CBCT devices, high-density materials and field of views. Clin Oral Implants Res 2017; 28: 1509-14.